

# *PDE Transform for signal, image and data analysis*

Yang Wang and Guowei Wei

**Department of Mathematics**

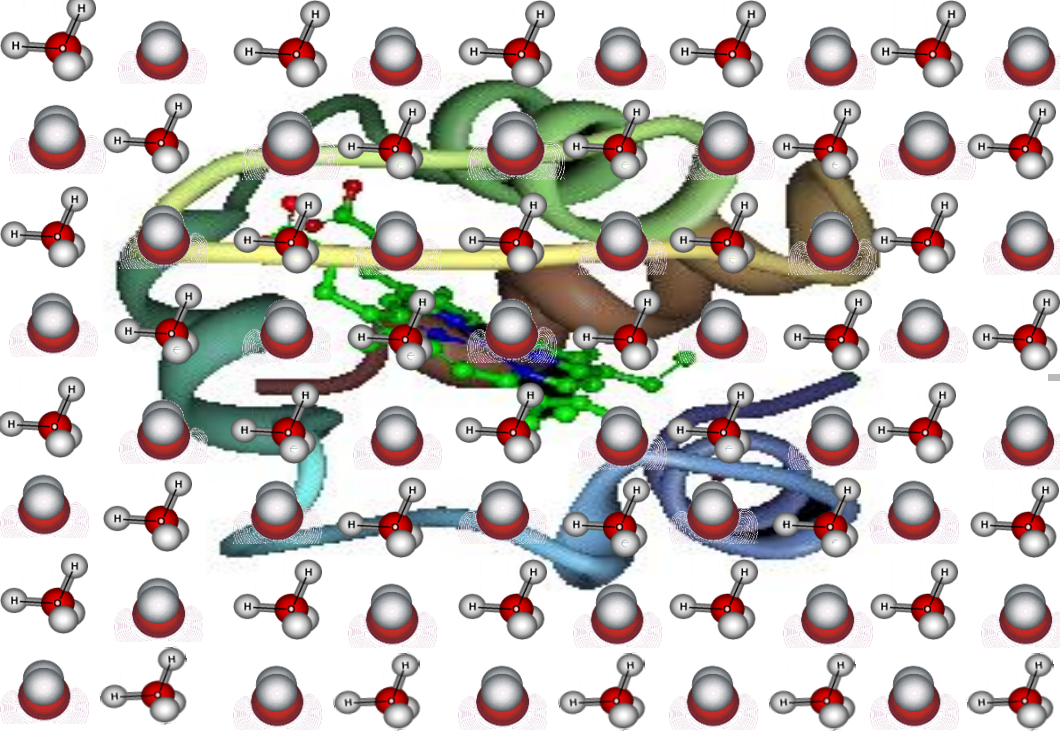
Yiying Tong

**Department of Computer Science and Engineering**

**Michigan State University**

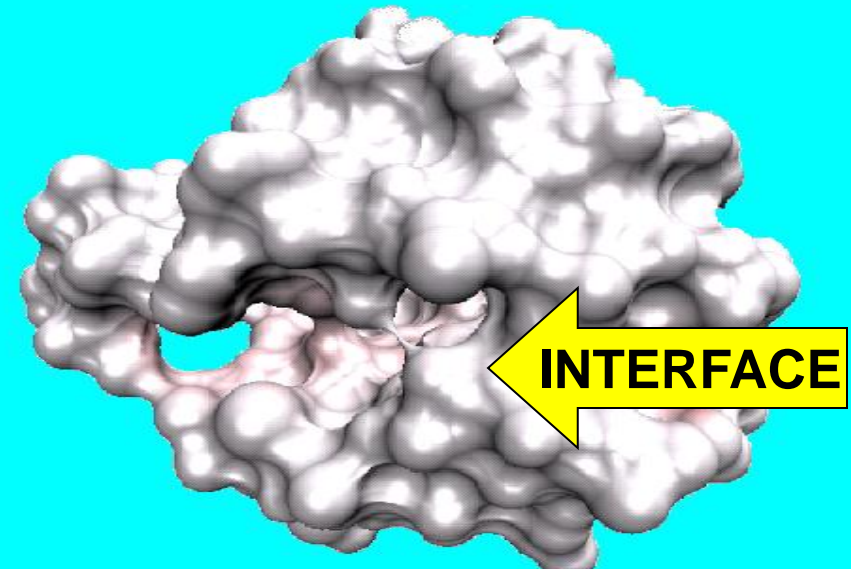
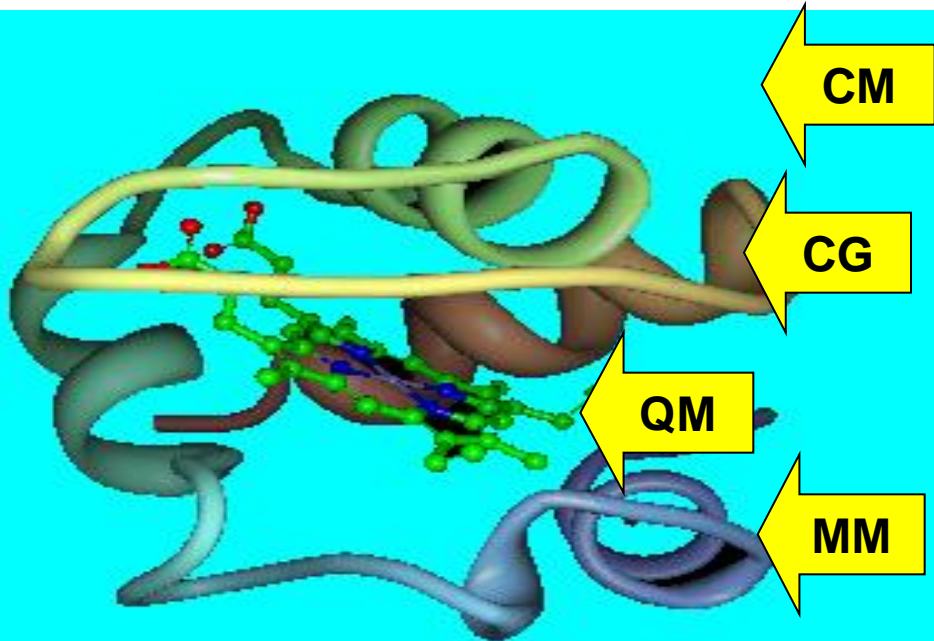
December 9, 2011, Gatech





## *Keyword Summary:*

- *Variational Multiscale/Differential geometry*
- *Continuum/Hydrodynamics*
- *Discrete/Molecular dynamics/QM*
- *Coarse graining /Stable manifold /Machine learning*
- *22 reviewed journal papers*



# Diffusion equation for image processing (Withkin 1983)

$$u_t(r,t) = d \nabla^2 u(r,t)$$
$$u(r,0) = I(r)$$

**Constant**

**Scale-space filter**  
**Gaussian filter**

**Original**



**Original+Noise**



**Processed with the  
diffusion equation**



# Perona-Malik equation (1990)

$$\frac{\partial u}{\partial t} = \nabla \bullet [d(|\nabla u|) \nabla u],$$

$$u(r, t=0) = I(r)$$

$$d(|\nabla u|) = \exp\left(-\frac{|\nabla u|^2}{2\sigma^2}\right), \quad or$$

$$d(|\nabla u|) = \frac{1}{1 + |\nabla u|^2}$$

Gradient dependent

Mean Curvature Flow

Original



# The First high-order stochastic geometric PDEs introduced for image analysis

Wei (1999); Greer & Bertozzi (2004); Gilboa, Sochen & Zeevi (2004); Xu and Zhou (2007); ....

$$\frac{\partial u}{\partial t} = \sum_{j=0} \nabla \bullet [d_j(|\nabla u|) \nabla \nabla^{2j} u] + P(|\nabla u|),$$

$$u(r, t=0) = I(r)$$

$$d_0(|\nabla u|) = \exp\left(-\frac{|\nabla u|^2}{2\sigma^2}\right),$$

$$\sigma^2 = \overline{|\nabla u - \overline{\nabla u}|^2}$$

Gradient dependent

Nonlinear term

Stochastic coef.

# Partial differential equation (PDE) transform

$$\frac{\partial u}{\partial t} = \sum_{i=0}^{n-1} \nabla \bullet [d_i(|\nabla u|) \nabla \nabla^{2i} u] + c_u(v - u),$$

$$\frac{\partial v}{\partial t} = \sum_{j=0}^{m-1} \nabla \bullet [d_j(|\nabla v|) \nabla \nabla^{2j} u] + c_v(u - v)$$

$$u(r, t=0) = v(r, t=0) = I(r)$$

Wang et al,  
IJNMBE 2011

## Intrinsic mode functions (IMFs)

$$w_{nm}^k = u_n - v_m = H_{nm} X^k, \quad \forall k = 1, 2, \dots$$

$$X_{nm}^1 = I(r)$$

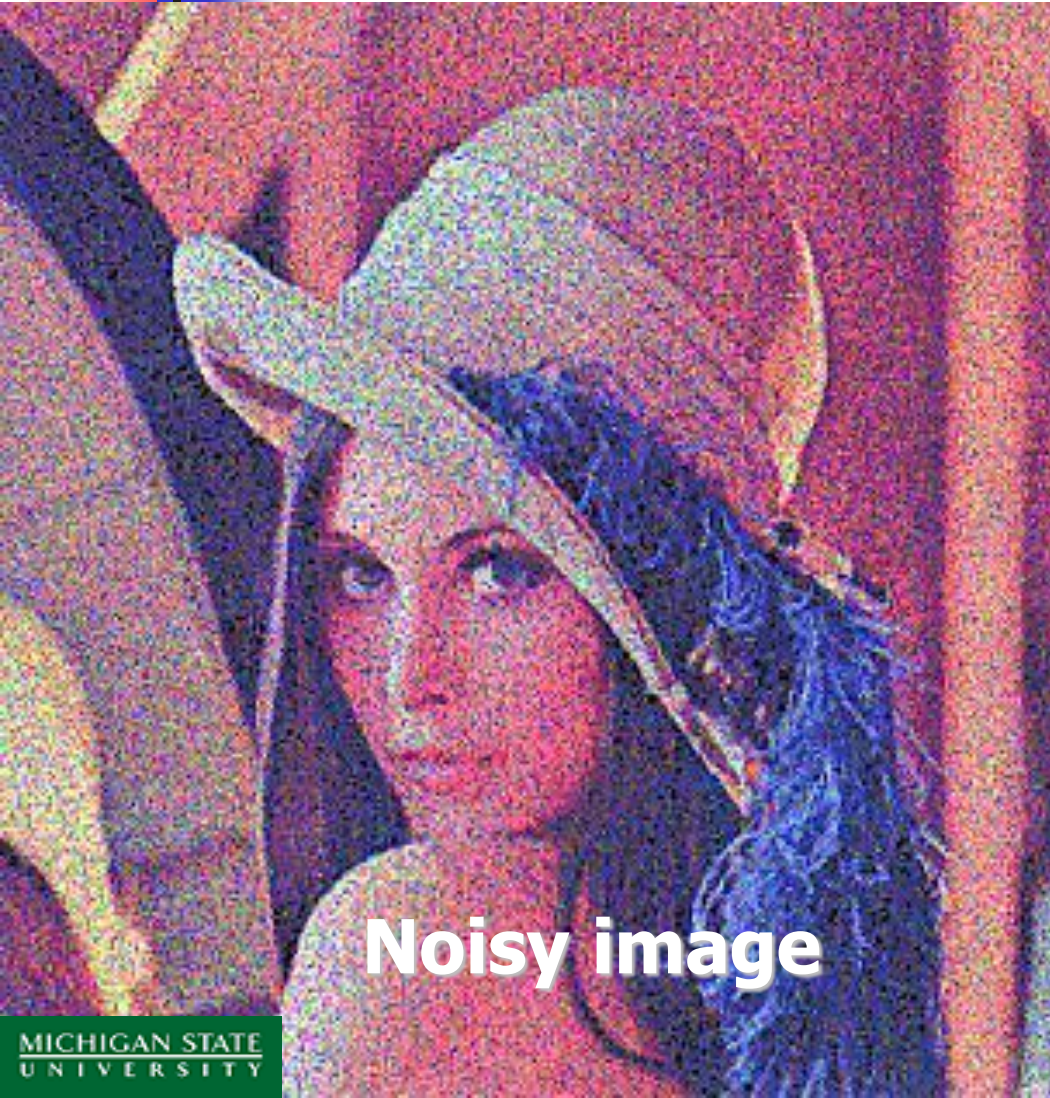
$$X_{nm}^k = X_{nm}^1 - \sum_{l=1}^{k-1} w_{nm}^l, \quad \forall k = 2, 3, \dots$$

$$I = X_{nm}^k + \sum_{l=1}^{k-1} w_{nm}^l$$

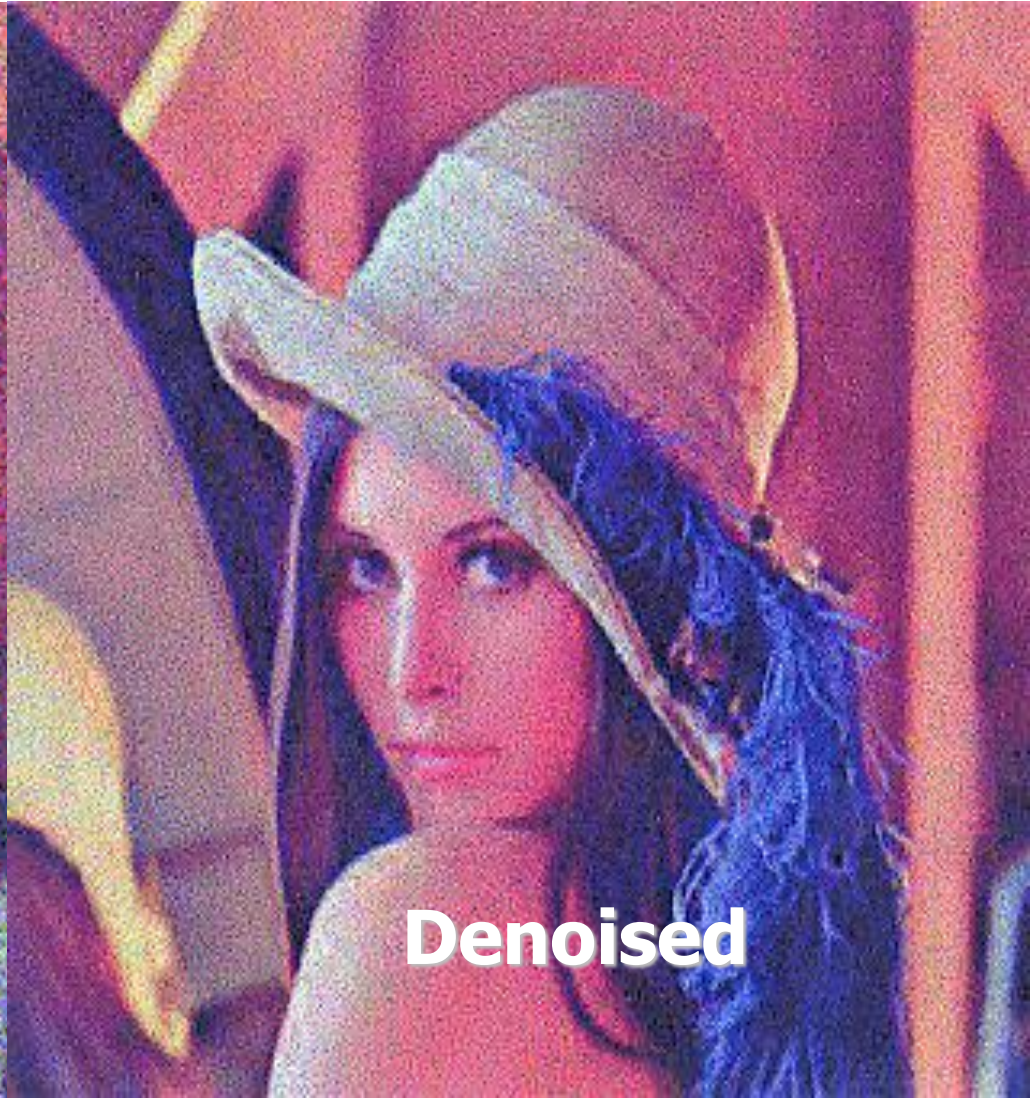
Perfect reconstruction

# Use of Cahn-Hilliard type of potential

$$\frac{\partial u}{\partial t} = \nabla \bullet [d_1(|\nabla u|) \nabla \nabla^2 u] + c(|\nabla u|)(u^2 - u_0^2)u$$



Noisy image

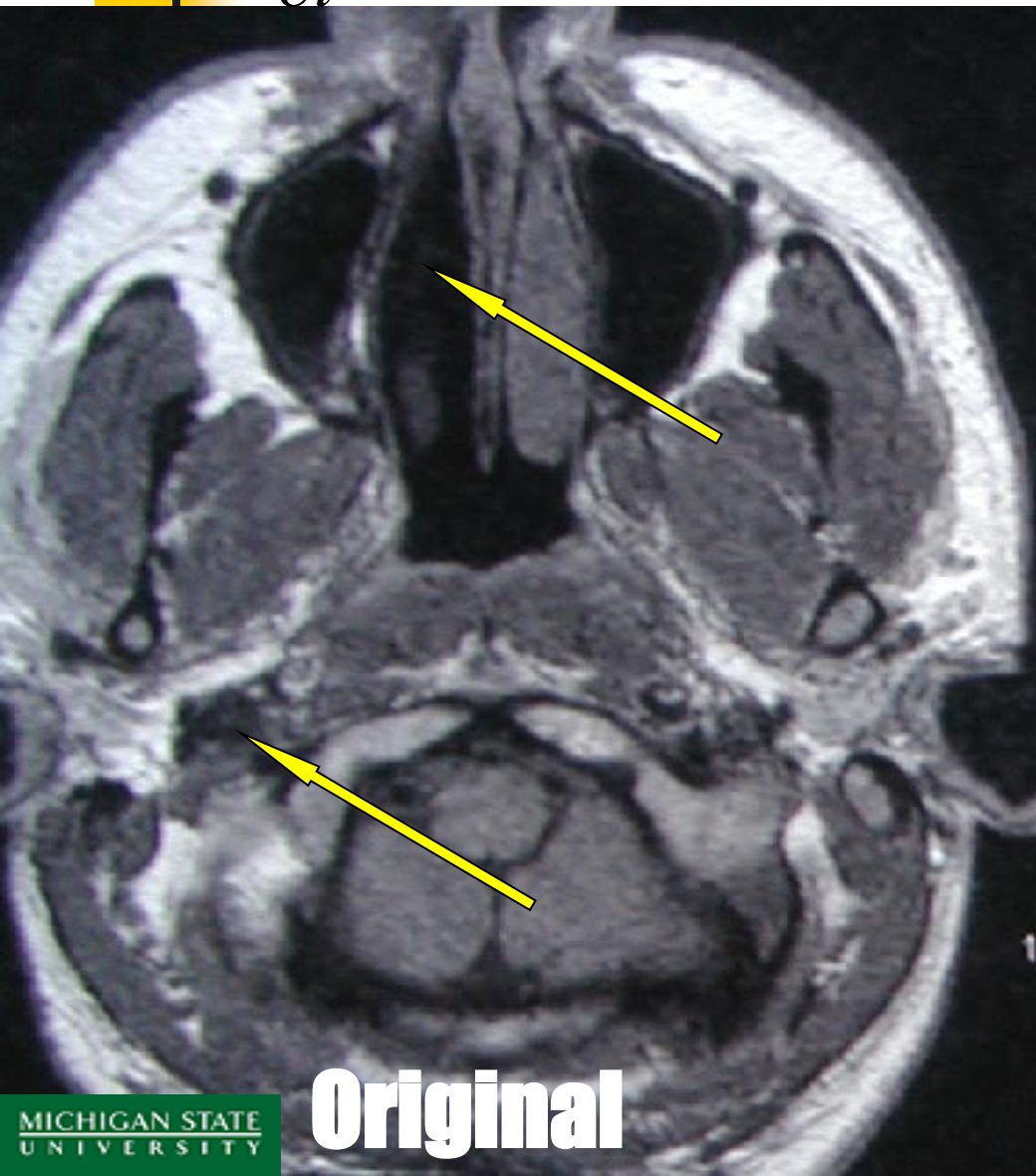


Denoised

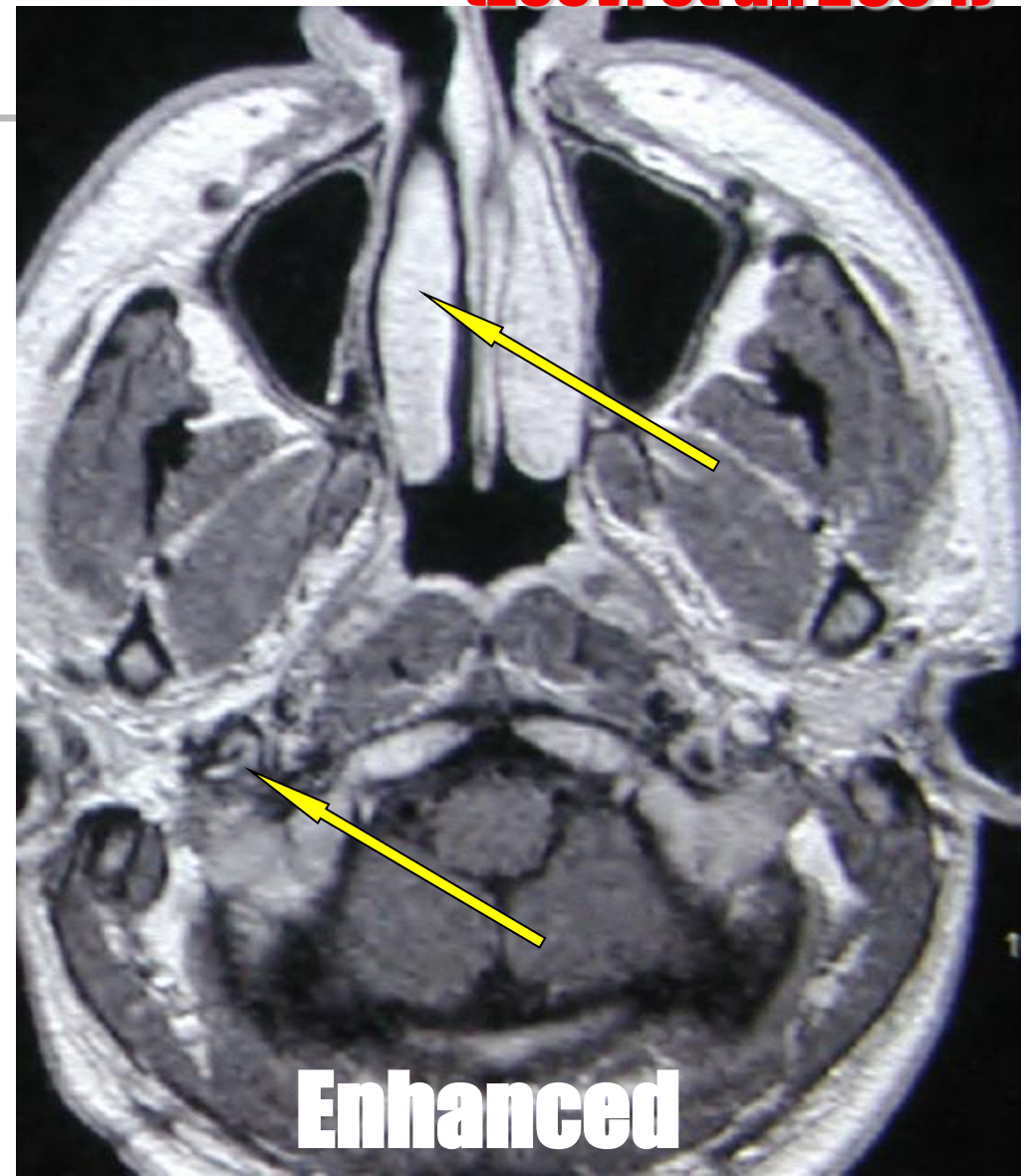
# Forward & Backward enhancement

$$\frac{\partial u}{\partial t} = \nabla \bullet [d_0(|\nabla u|)\nabla u] + \nabla \bullet [d_1(|\nabla u|)\nabla \nabla^2 u]$$

(Zeevi et al. 2004)

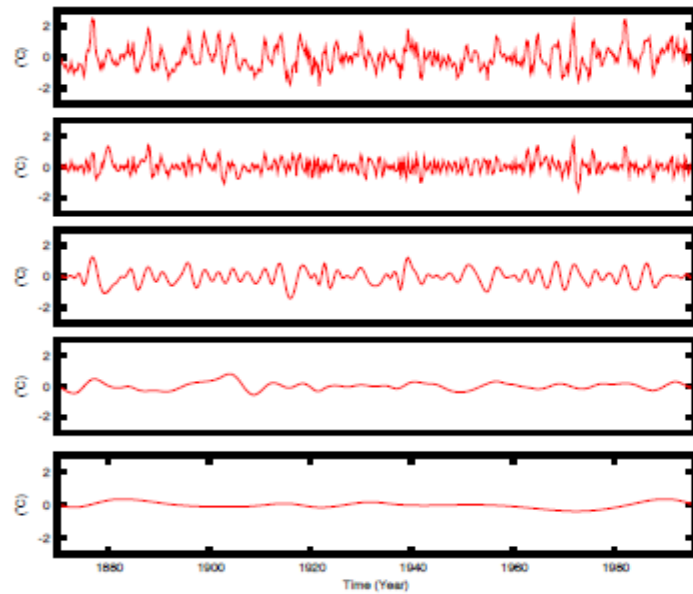
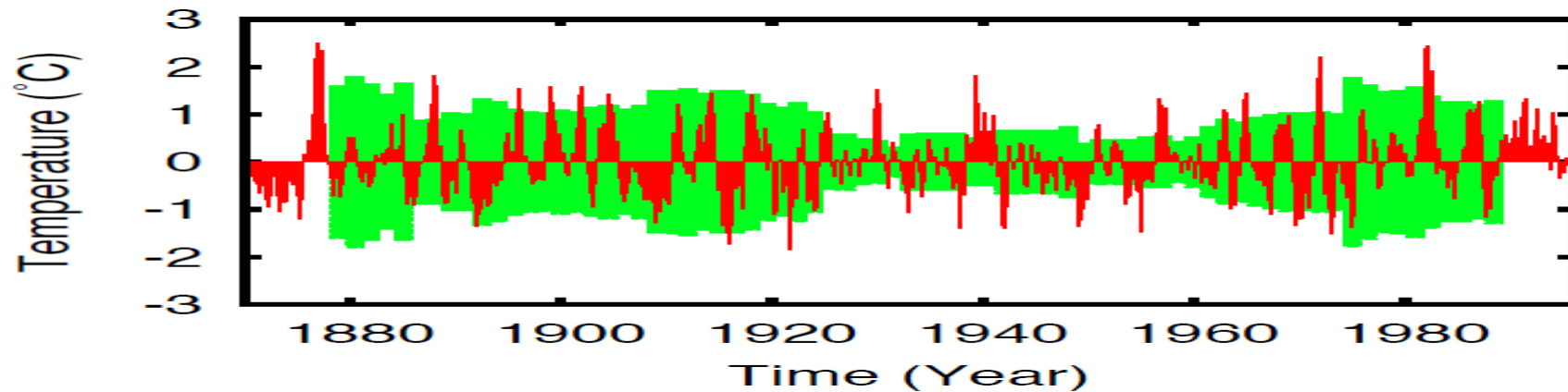


Original

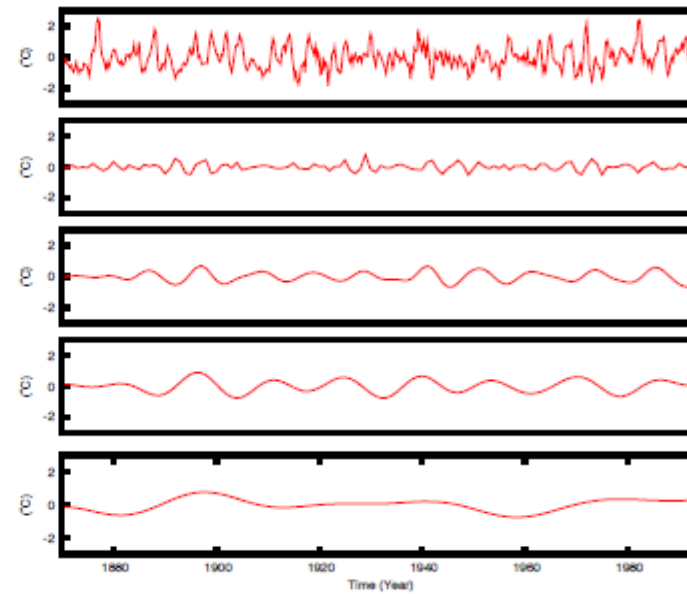


Enhanced

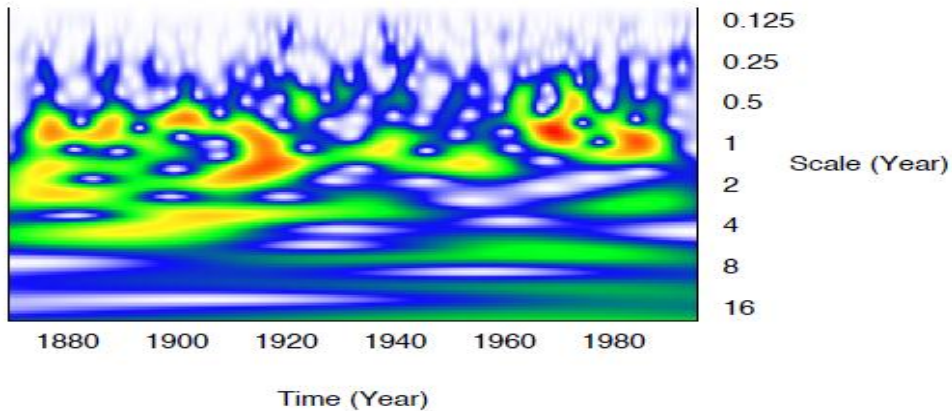
# Central Pacific sea surface temperature



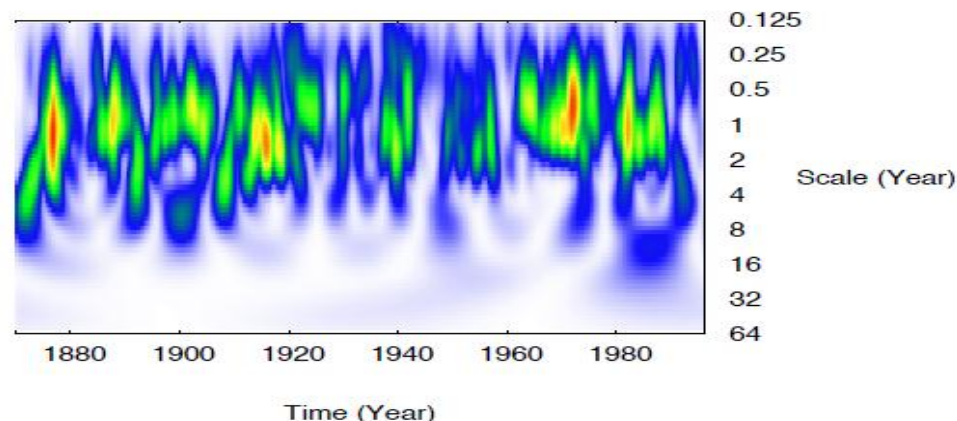
(a) The original SST signal (top panel) and the first four significant intrinsic mode functions generated by the EMD method.



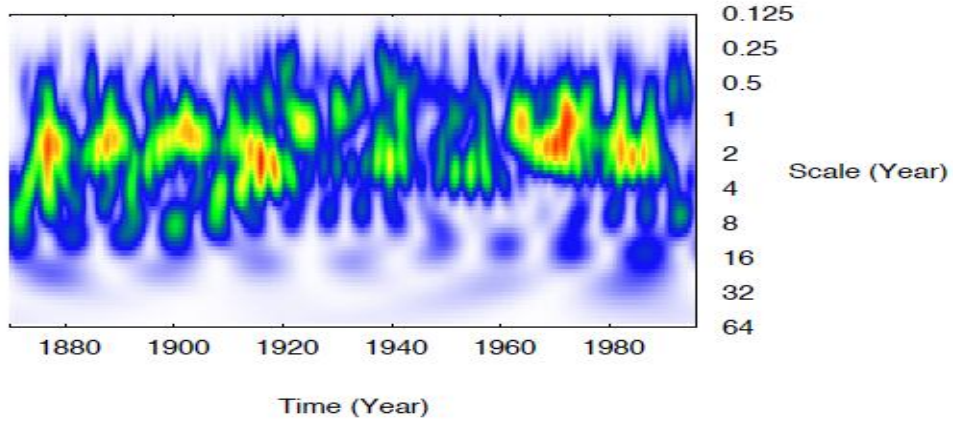
(b) The four modes generated by the PDE transform for the same SST signal on the top panel are similar to those from the EMD decomposition.



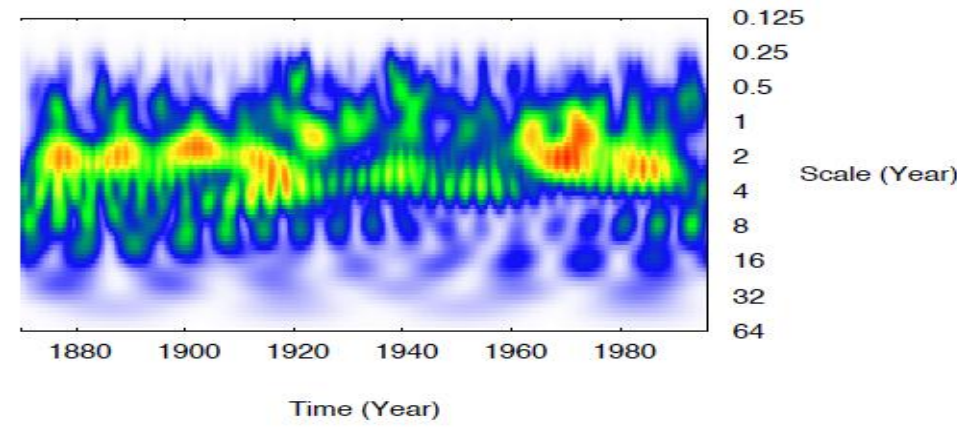
(a) Continuous wavelet analysis of the SST Nino3 data.



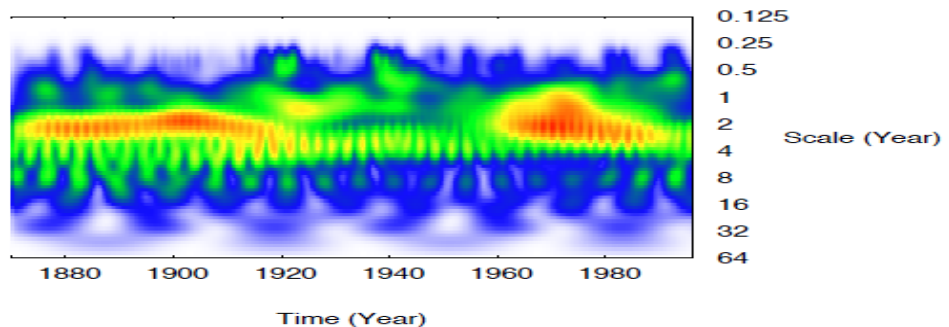
(b) PDE transform using 2nd order PDE.



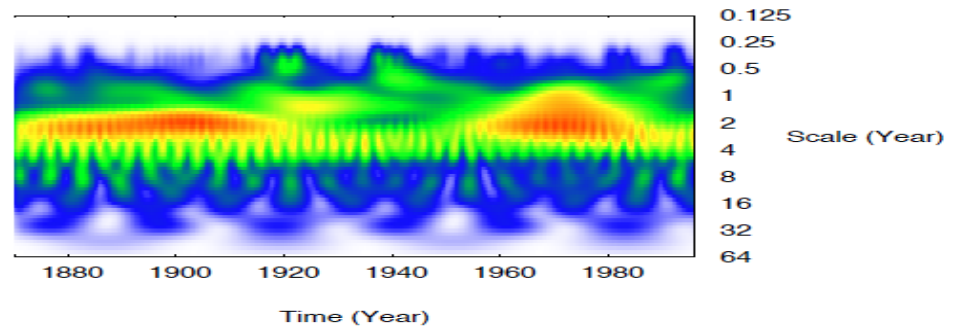
(c) PDE transform using 4th order PDE.



(d) PDE transform using 8th order PDE.

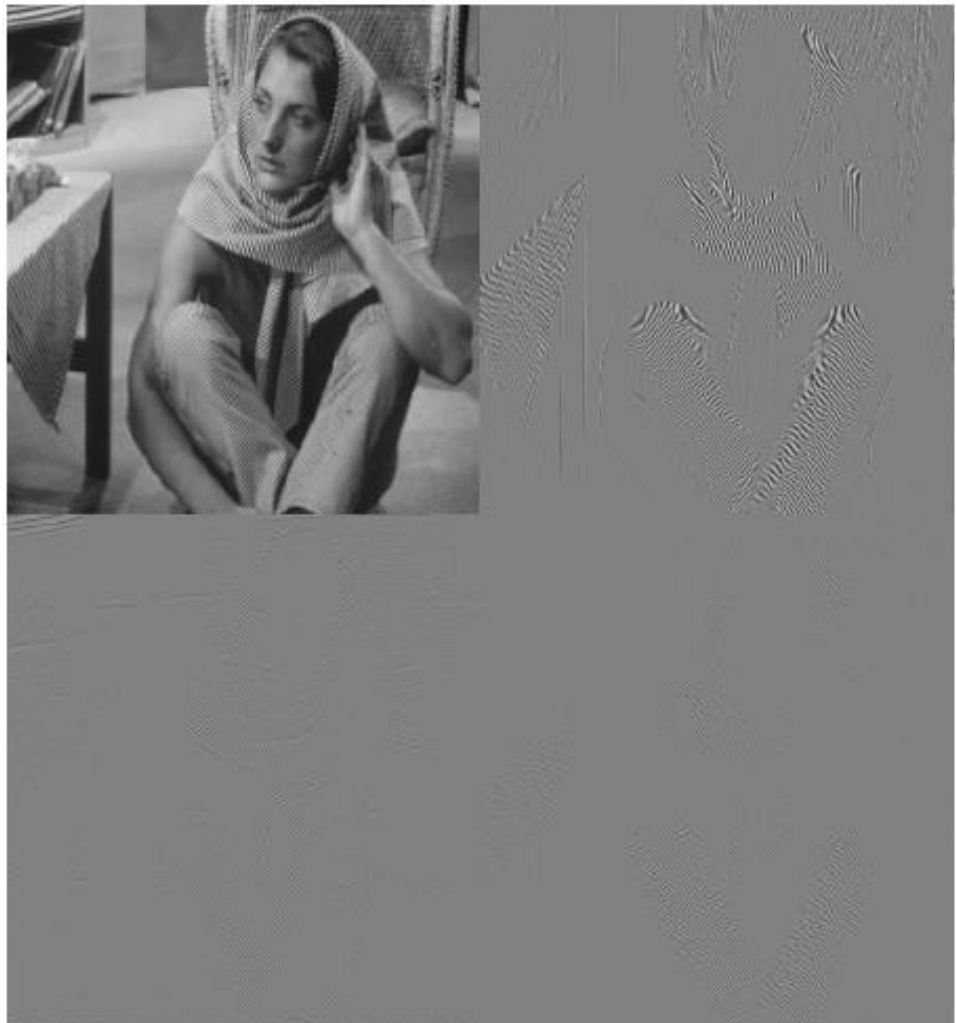


(e) PDE transform using 20th order PDE.



(f) PDE transform using 40th order PDE.

# Wavelet transform vs PDE transform



(a) Discrete wavelet decomposition of the Lena image.



(b) PDE transform (using 2nd order PDE) of Barbara image.

# PDE transform based local statistical analysis

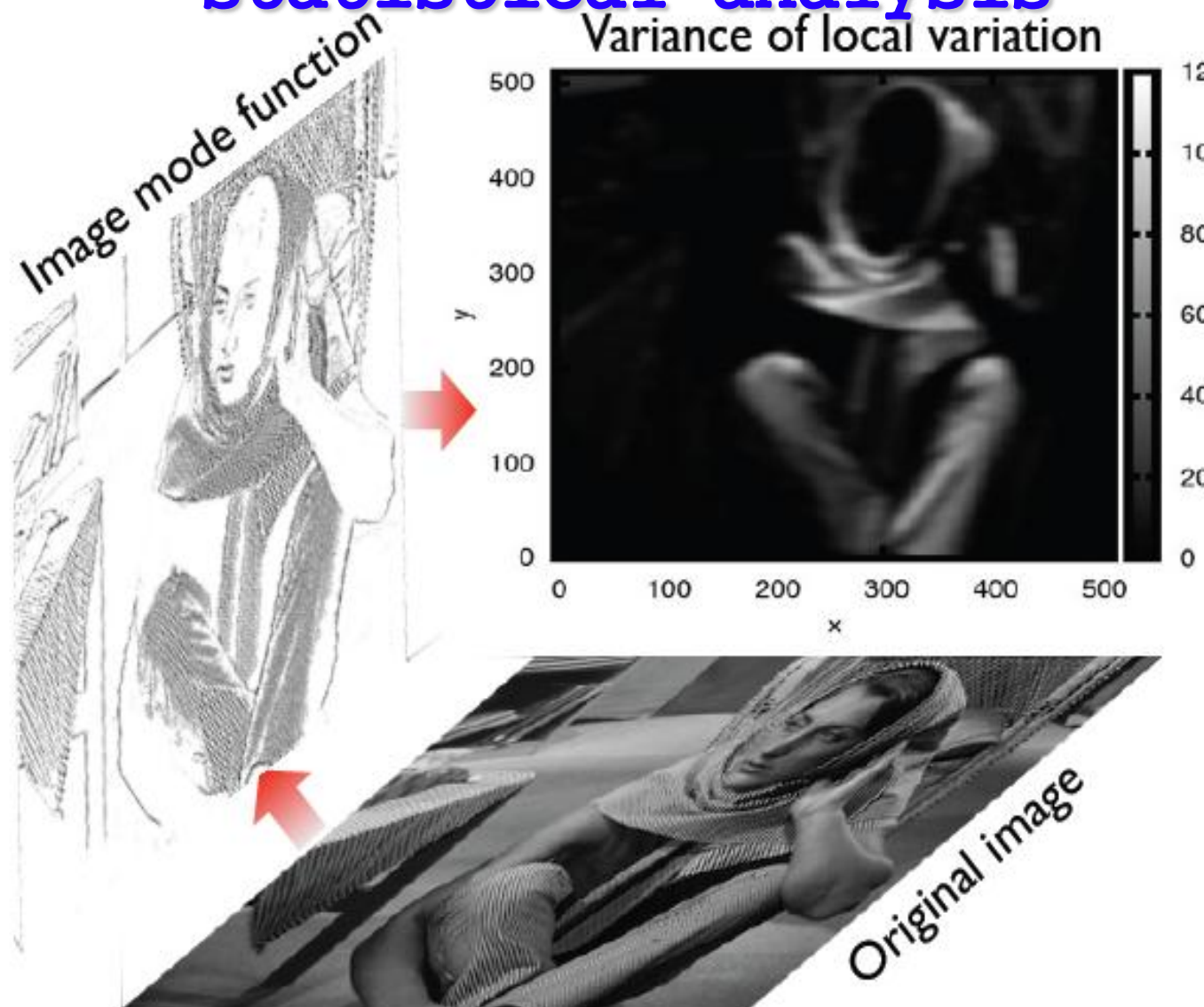
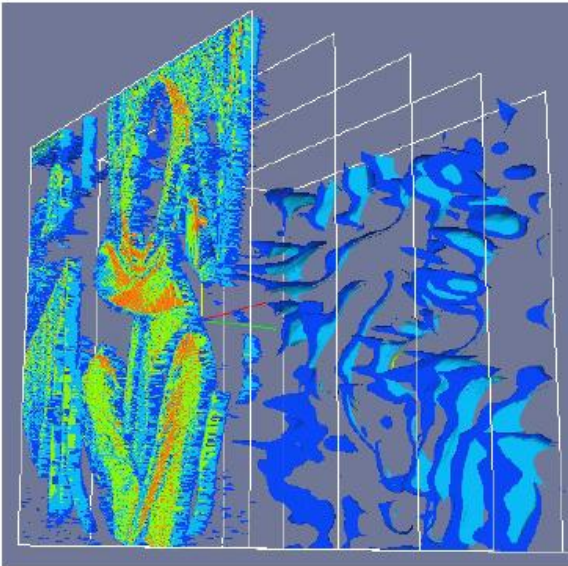


Figure 4: Adaptive PDE transform for selective texture extraction in the Barbara image. The variance of the local variation is shown in the top chart.

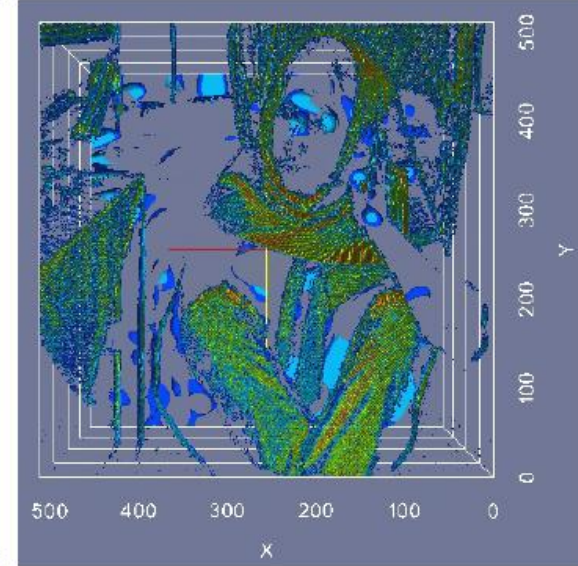
# PDE transform based correlations



(a) Original Barbara image.



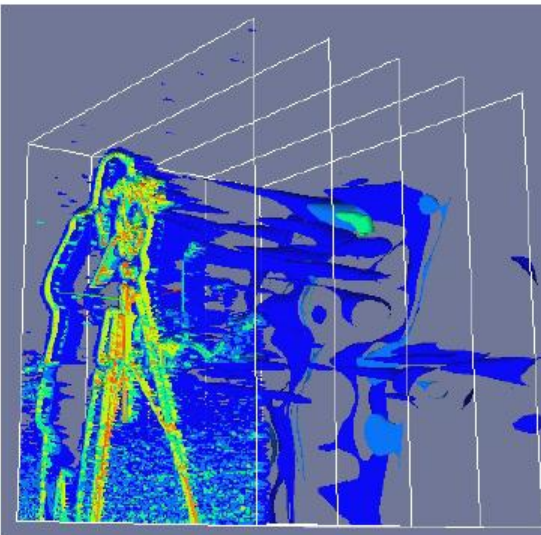
(b) 4D density of the Barbara image.



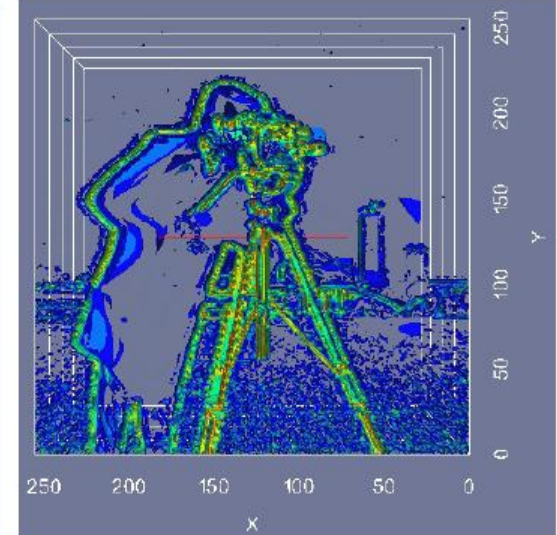
(c) Front view of the Figure 8(b).



(d) Original camera man image.



(e) 4D density of the camera man image.



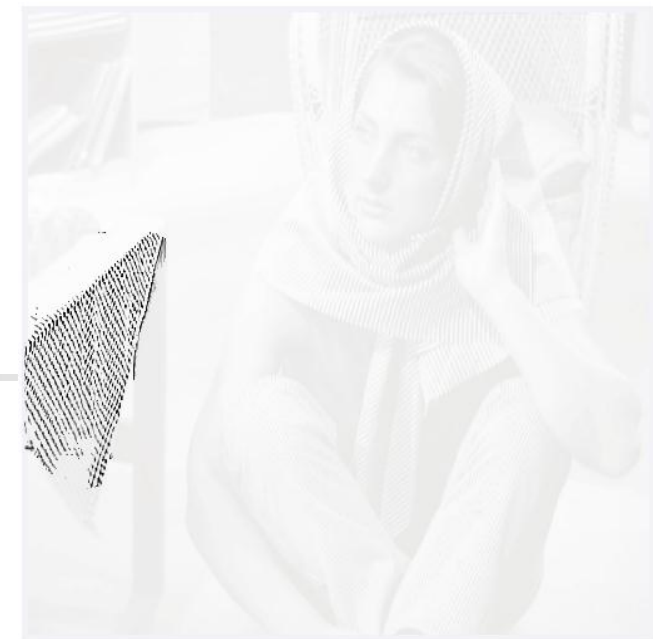
(f) Front view of the Figure 8(e).



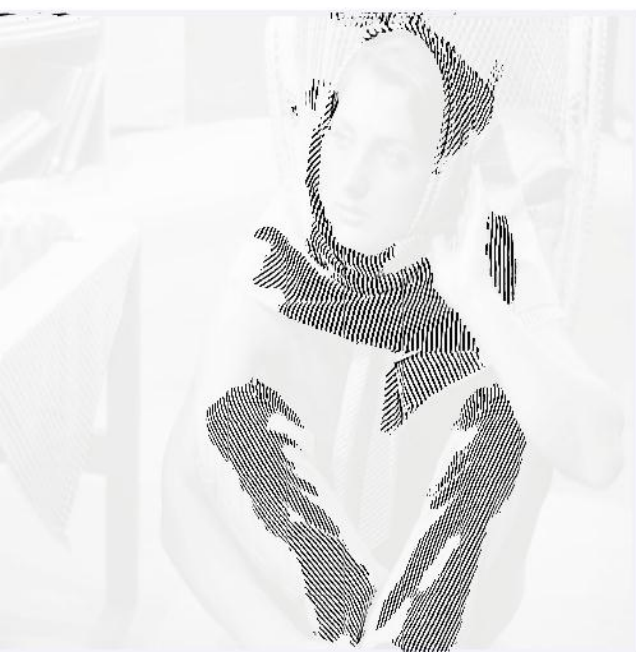
(a) Original image.



(b) Image mode function.



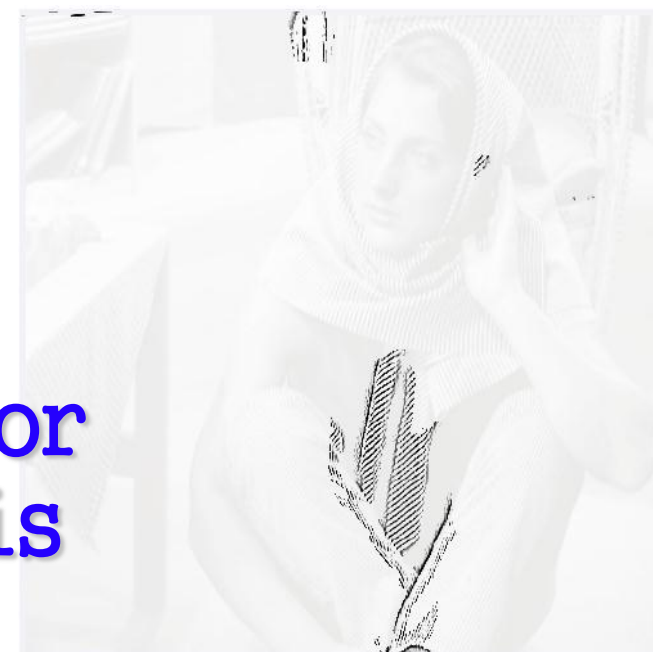
(e) Texture 3



(c) Texture 1



(d) Texture 2



(f) Texture 4

PDE transform for  
texture analysis

# PDE transform for texture analysis



(a) Original image.



(b) Mode function.

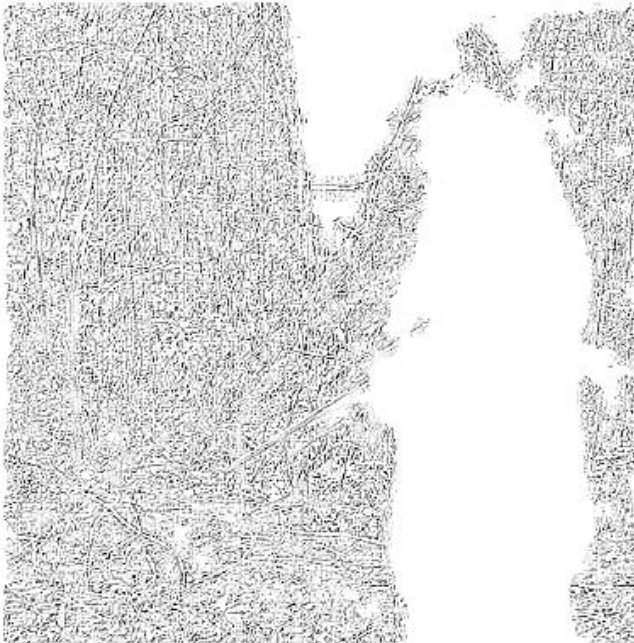


(c) Extracted texture.

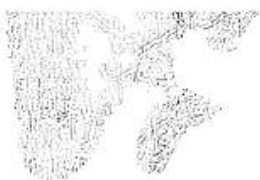
Figure 3: Extraction and separation of texts, background watermark, and textures of image 3(a). Shown in the 3(b) and 3(c) are the image mode function and extracted texture using the proposed adaptive PDE transform.



(a) Original image.



(b) Texture 1

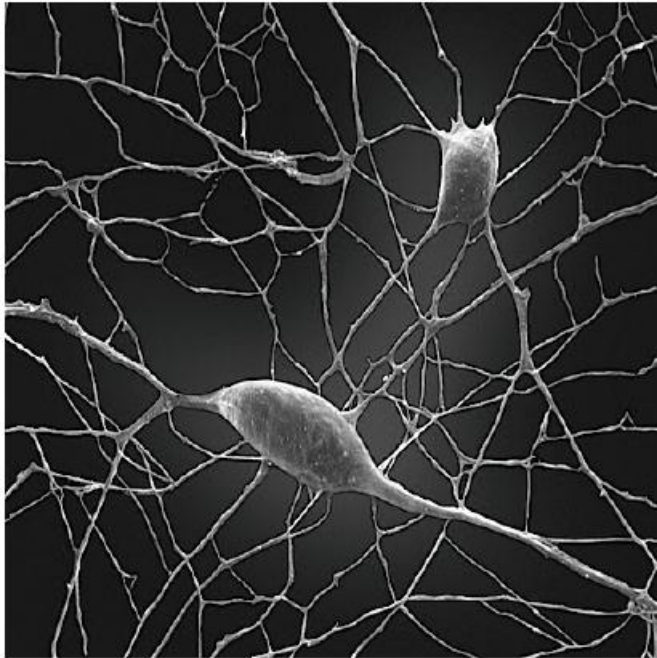


(c) Texture 2



(d) Texture 3

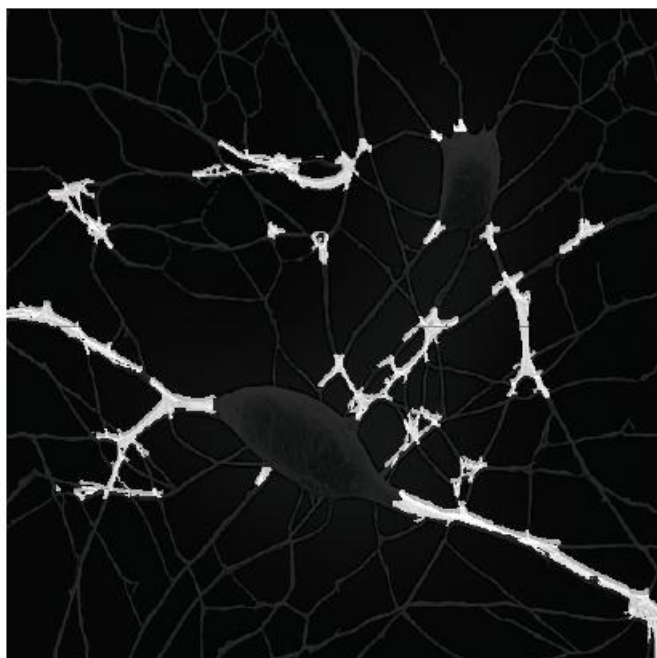
PDE transform  
for sniper  
identification



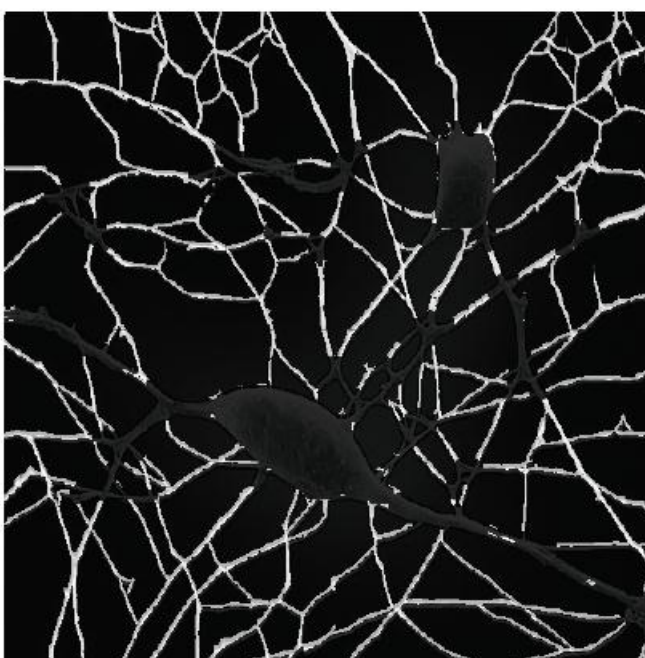
(a) Original neuron image.



(b) Class 1 of the selective neuron skeleton.



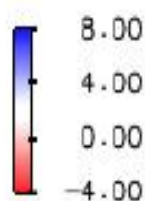
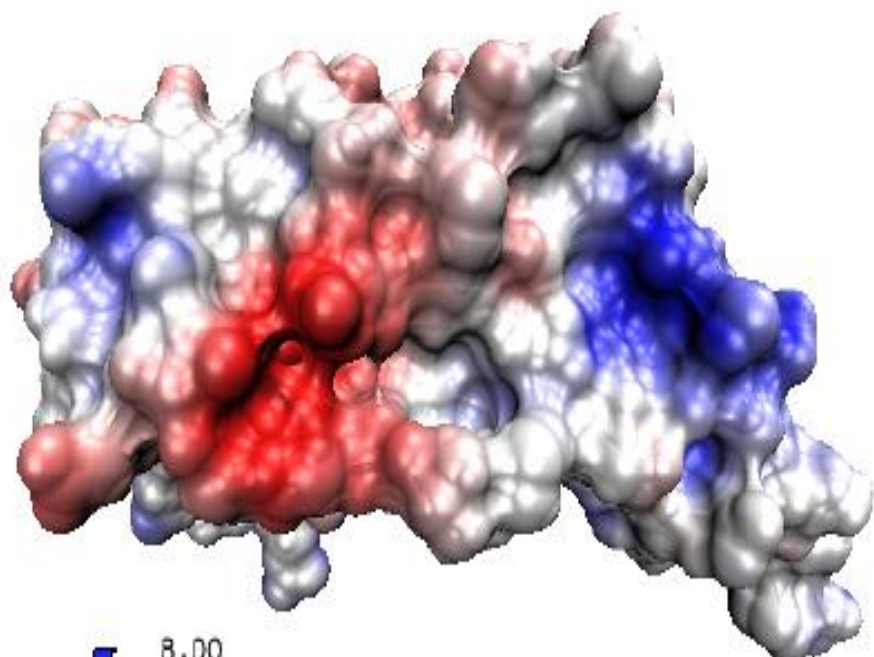
(c) Class 2 of the selective neuron skeleton.



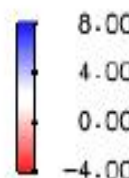
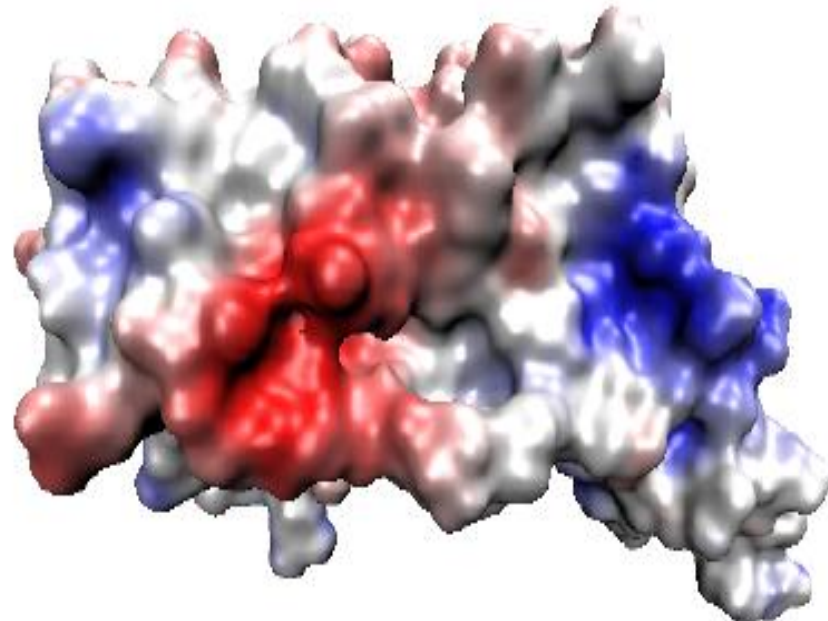
(d) Class 3 of the selective neuron skeleton.

PDE transform  
for neuron  
classification

# PDE transform for protein surface construction



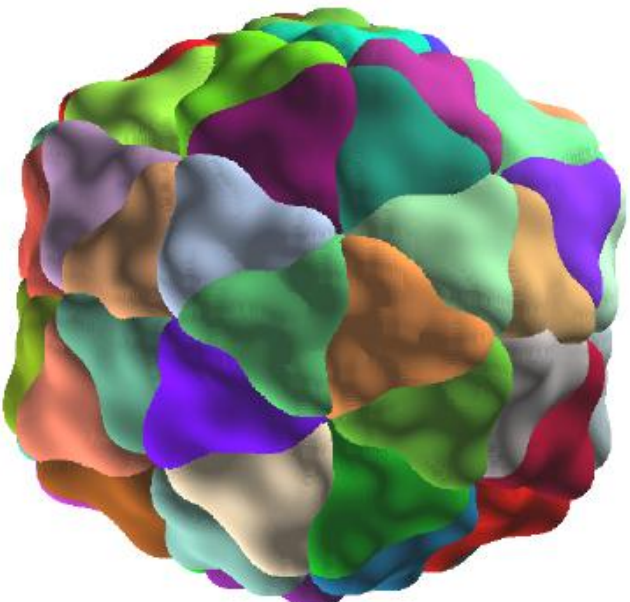
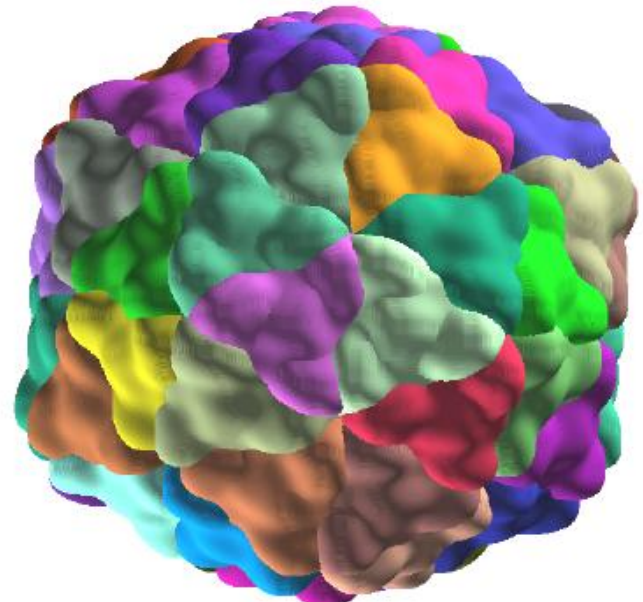
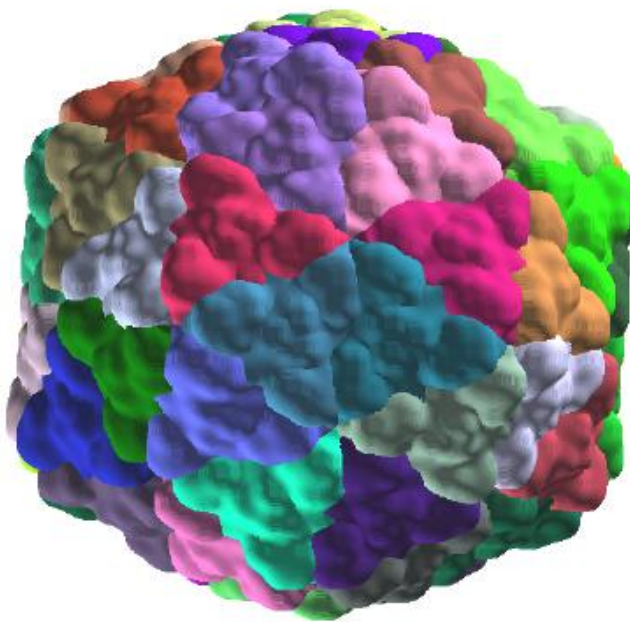
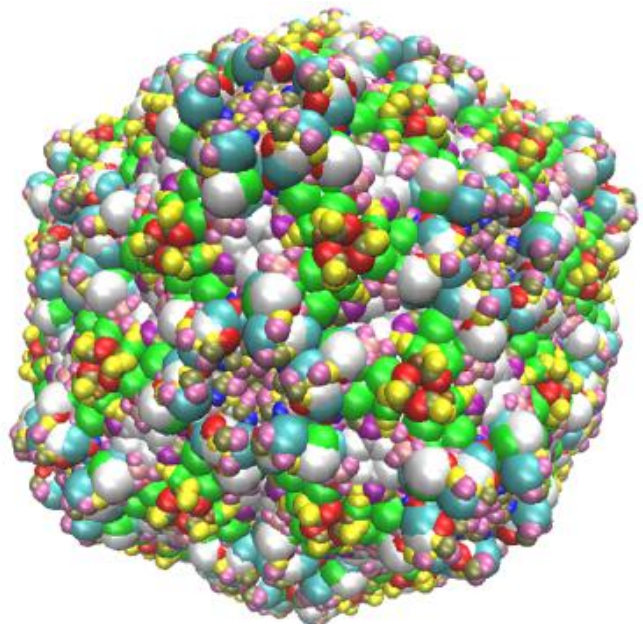
(a)

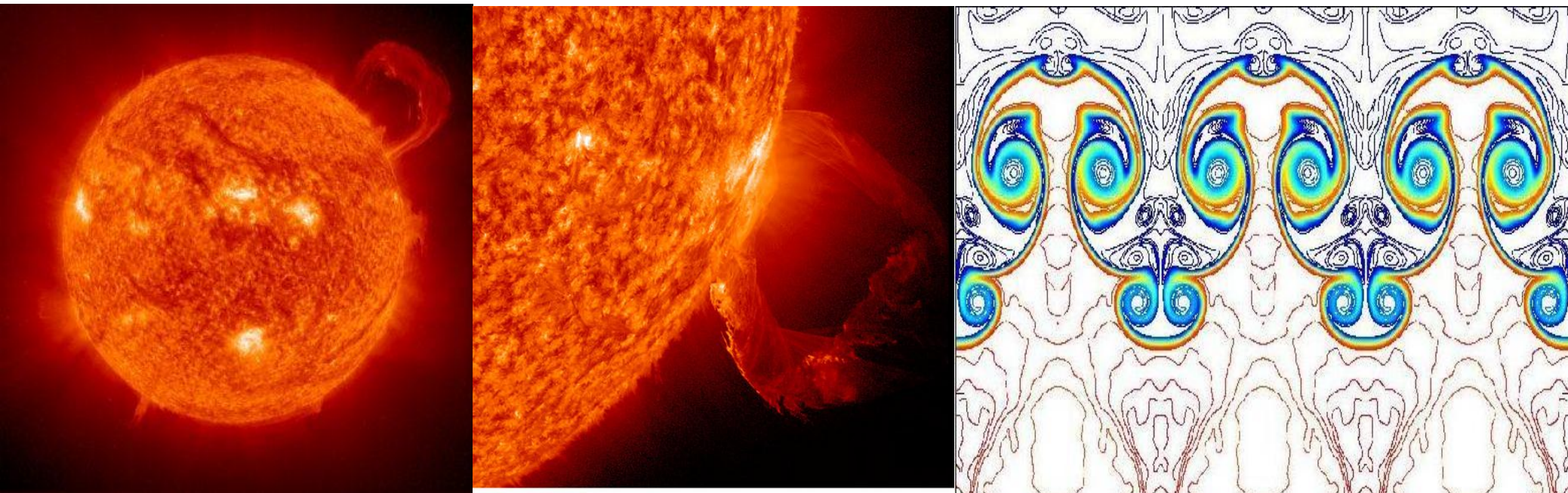


(b)

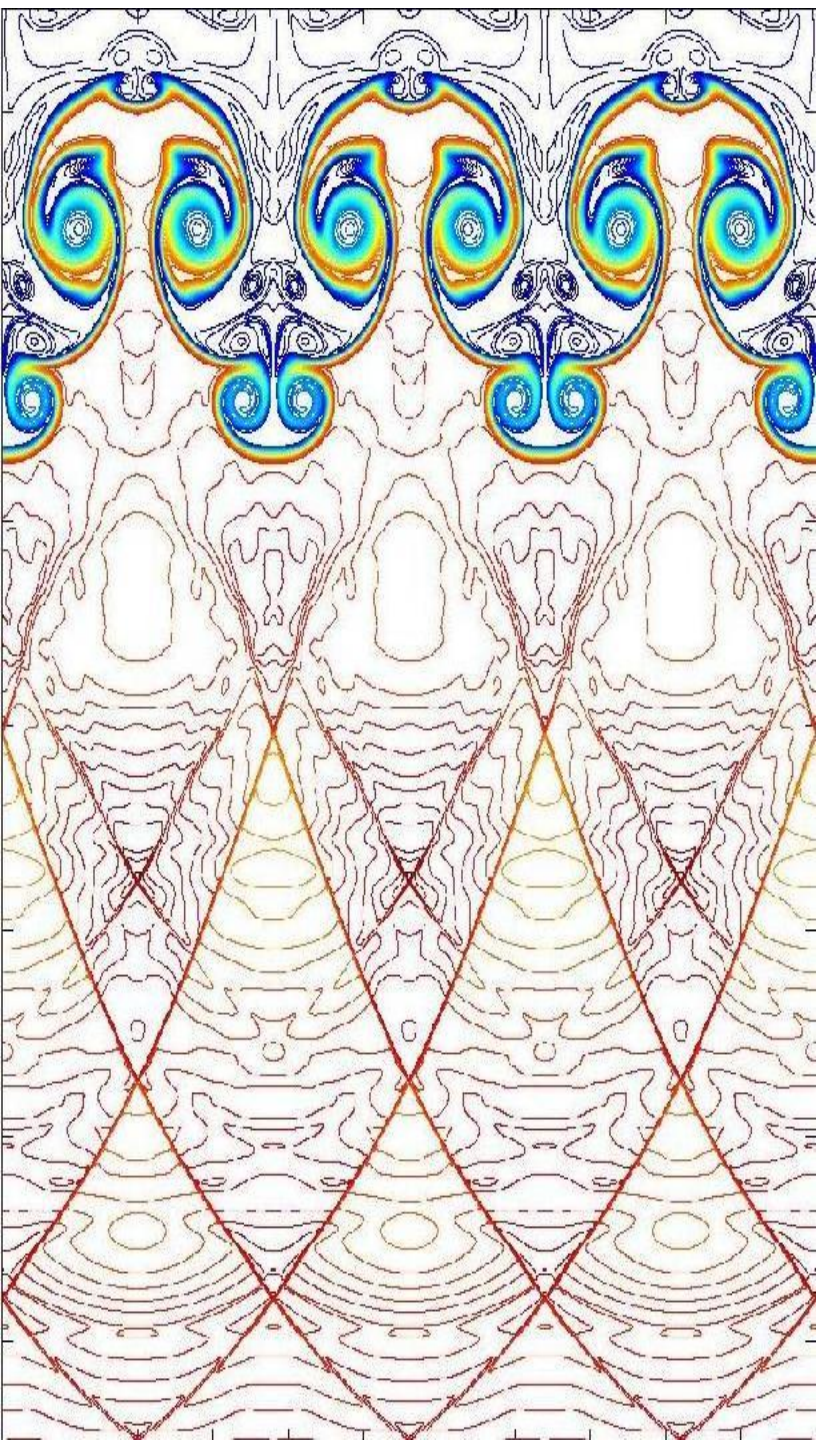
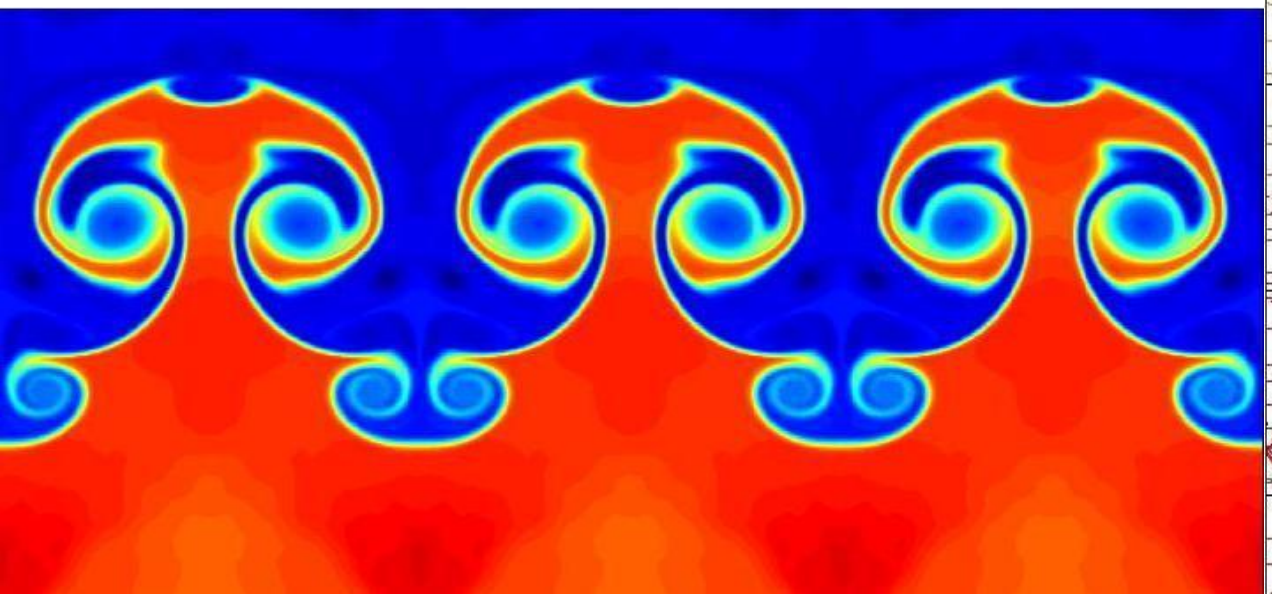
Figure 13: Electrostatic surface potentials for protein 1a7m mapped on two surfaces. (a) Surface generated by MSMS; (b) Surface generated by the 12th order PDE transform.

PDE  
transform  
for  
multiscale  
analysis





## Richtmyer-Meshkov instability



# Comparison of Hilbert-Huang, wavelet, Fourier and PDE transforms

- Only yield the relevant functional modes
- Each mode contains desired frequency range
- Mode is extracted using accurate high order PDEs based band-pass filters
- Each sub-band width is totally controllable
- Each mode function is determined by PDE order and evolution time
- Adjustable dual temporal-frequency localization
- Each mode contains selected frequency range
- Physical domain representation
- Applicable for non-stationary signal, and no Gibbs oscillations

## Partial Differential Equation Transform

### Hilbert-Huang transform

- Each mode is obtained by spline based lowpass filter
- Instantaneous frequency is obtained for characterizing non-stationary data

### Wavelet transform

- Dual time-scale analysis
- Robust choice of the mother wavelet
- Dilation and translation are used to capture the local characteristics

### Fourier transform

- Perfect localization in frequency space
- Gibbs oscillations
- Impressive improvements and applications are still occurring